

COS FUV Focus Determination for the G140L Grating

Parviz Ghavamian

¹*Space Telescope Science Institute, Baltimore, MD*

October 03, 2012

ABSTRACT

The procedures for determining the COS FUV fine-focus for the G140L grating from a dedicated Cycle 17 Supplemental Calibration program are described. The minimum in the focus curve (and hence the optimal focus offset) is found to lie at -410 focus steps from the current nominal focus position. However, the focus curve for this grating is found to be broad and shallow, which combined with the uncertainty in repeatability make spectra taken at the nominal focus position indistinguishable from spectra taken close to the derived optimum offset. It is concluded that the current default focus position determined for the G140L grating during SMOV remains valid, and no further adjustment of the focus offset is recommended.

Contents

- Introduction (page 2)
- Focus Sweep Observations (page 2)
- Post-Processing (page 3)
- Analysis (page 5)
- Conclusions (page 8)
- Acknowledgments (page 8)
- References (page 8)

1. Introduction

In this report, we describe the analysis and conclusions relating to the determination of the G140L grating focus of the COS FUV channel during the Cycle 17 Supplemental Calibration program of HST.

During SMOV, the optimal focus offsets for the G130M and G160M gratings were initially determined via a focus sweep using stars with narrow absorption lines. The optimal setting was determined by measuring absorption line widths in the spectra at different focus settings, then fitting a parabola to the FWHM of absorption lines in that spectrum (or autocorrelation FWHM) as a function of focus position. However, subsequent science observations with COS showed that the G130M and G160M spectra were still out of focus. The focus sweep was performed again on a different set of stars featuring a broader range of absorption lines. This time, both autocorrelation and Fourier transform techniques were used on spectra of the chosen stars to determine the optimal focus setting (Lennon et al. 2010). This approach allowed a robust and consistent estimate of the optimum focus setting for G130M and G160M, and the resulting computed offsets were implemented into the flight software for COS.

The initial focus sweep performed during SMOV for the G140L grating was not repeated, though an autocorrelation analysis of the existing focus sweep data for that grating (observations of the QSO H1821+643 from SMOV program 11484) showed the optimal focus offset was +100 steps from the nominal position (Lennon et al. 2010). The focus position for the G140L grating was therefore set to -370 motor steps for the 1105 Å setting and +30 motor steps for the 1230 Å setting. However, the G140L focus curve was considerably broader and shallower than the curve for the medium resolution gratings. Further analysis of the H1821+643 data after the focus change showed that the uncertainty in optimal focus position was larger than 200 steps for G140L, unlike the medium resolution gratings where the optimal focus setting was determined to within 50 focus steps. Therefore, a Cycle 17 Supplemental calibration program was initiated to observe a more suitable target with the G140L grating, with the goal of obtaining a more accurate estimate of the optimum focus position.

2. Focus Sweep Observations

The G140L focus sweep was performed as part of the Cycle 17 Supplemental Calibration Program (PID 12080) and used the B2 star AzV 18 in the Small Magellanic Cloud ($V=12.5$). The observations were performed in one visit, at a central wavelength setting of 1105 Å. The exposure IDs for the data used in the analysis are listed in Table 1. The focus sweep consisted of a short nominal exposure at the default focus position of -370 motor steps relative to the HST secondary mirror for G140L/1105 Å. This was followed by a commanded focus offset of -800 steps relative to the nominal position and an exposure at that focus position, followed by additional focus offsets in units of +100 focus steps and exposures at those positions.

The focus sweep extended out to a commanded focus offset of +700 steps, passing through the nominal focus. After the exposure at +700 offset focus steps, the focus was reset to its nominal focus where a final exposure was taken. Specified in this manner, the focus sweep included three exposures at the nominal default focus position, a redundancy designed to characterize the repeatability of the focus offset (and hence estimate the uncertainty in optimal focus position). The tagflashes were specified to occur at 100s intervals for a duration of 10s each, in order to maximize the ability to correct for OSM drift (and hence minimize the impact of the drift on the spectral resolution of the data). For the 1105 Å setting, the G140L observations are restricted to Segment A and have useful data over a wavelength range of 1122 Å – 2000 Å.

3. Post-Processing

The presence of fixed pattern structure (grid wire shadows, dead spots, etc) in the data is problematic. The fixed pattern noise produces dips and notches in the extracted one-dimensional spectra, causing confusion in the identification of spectral lines and adding noise to the derived focus curves. The fixed pattern noise is stationary on the detector, while the dispersed spectrum shifts on the detector as the focus is changed. This makes features such as the grid wires move about in wavelength space in the extracted one-dimensional spectra. Normally the fixed pattern noise is mitigated during pipeline processing by combining exposures from multiple FPPOS positions. However, all of the spectra from program 12080 were acquired at the default FPPOS=3 setting, precluding this approach. Therefore, the fixed pattern noise was removed by setting FLATCORR=YES in CalCOS 2.13.6 and specifying a two-dimensional flat field constructed from a one-dimensional template. The latter was generated by S. Beland of the COS IDT, using G140L data acquired in Cycle 17 Calibration Program 12086 (D. Massa, PI). The flat field was highly effective in removing the fixed pattern noise from the spectra.

The focus analysis was performed on spectra obtained from summing each of the *_flt.fits files in cross-dispersion. The sum was carried out between the lower and upper cross-dispersion pixels specified by the spectral extraction reference file (*_1dx.fits) for G140L. No background subtraction was applied to the extracted spectra, which were in corrected detector coordinates (XCORR and YCORR).

Exposure ID	Exptime (s)	Absolute Focus Setting*	Focus Offset	Breathing-Corrected Focus Offset
lbeg01e3q	150	-372	0	79
lbeg01e5q	500	-1173	-801	-829
lbeg01e7q	700	-1074	-702	-699
lbeg01e9q	700	-975	-603	-562
lbeg01ebq	700	-874	-502	-433
lbeg01edq	700	-773	-401	-434
lbeg01efq	700	-675	-303	-302
lbeg01ehq	700	-574	-202	-162
lbeg01ejq	700	-473	-101	-45
lbeg01elq	700	-372	0	-37
lbeg01enq	700	-272	+100	96
lbeg01epq	700	-171	+201	230
lbeg01erq	700	-70	+302	359
lbeg01etq	700	31	+403	365
lbeg01eyq	700	132	+504	495
lbeg01f3q	700	232	+604	633
lbeg01f5q	700	331	+703	757
lbeg01f9q	600	432	+804	769
lbeg01fdq	700	-372	0	-8

Table 1. Exposure information for the G140L focus sweep. The absolute focus setting is recorded in the LOMFSTP keyword in the *_spt.fits file. Error in the Breathing-Corrected Focus Offset is +/-1 steps.

Before analyzing the characteristics of the absorption lines, the estimated focus position for each exposure was corrected for OSM breathing using the HST focus breathing tool (<http://focustool.stsci.edu/cgi-bin/control.py>). The breathing model used for the calculation was that of ACS/WFC1, which used the start and stop time of each exposure to predict an average breathing offset for the HST secondary mirror in microns. For a calculated breathing offset of m microns, the corrected focus offset F_{corr} is

$$F_{corr} = F - 21.1 * m$$

where F is the focus position estimated from the telemetry (the LOMFSTP parameter listed in the support file). The breathing-corrected focus offsets for each exposure from the focus sweep are shown in Table 1. With the breathing correction, some of the exposures in the focus sweep begin to overlap in focus position (for example, the

spectra with specified offsets of -500 and -400 steps both end up at a focus offset of close to -433 steps once breathing is taken into account; see Table 1).

4. Analysis

The G140L spectra of AzV 18 include broad stellar absorption lines, as well as intrinsically narrow Galactic and SMC absorption lines. However, the broad lines are either resolved or barely resolved in the spectra, while the narrow lines typically arise from multiple components (Galactic and SMC) close enough together to be unresolved at the resolution of the G140L grating. Examination of absorption line cores from across the spectrum of AzV18 showed that increasingly negative focus offsets beyond -500 and increasingly positive focus offsets beyond +100 could be ruled out immediately. An example is shown in Figure 1, where a pair of C II λ 1335 Å absorption components are barely resolved from one another in COS spectra at focus offsets between -500 and +100 (excluding breathing correction), but are completely blended outside that range.

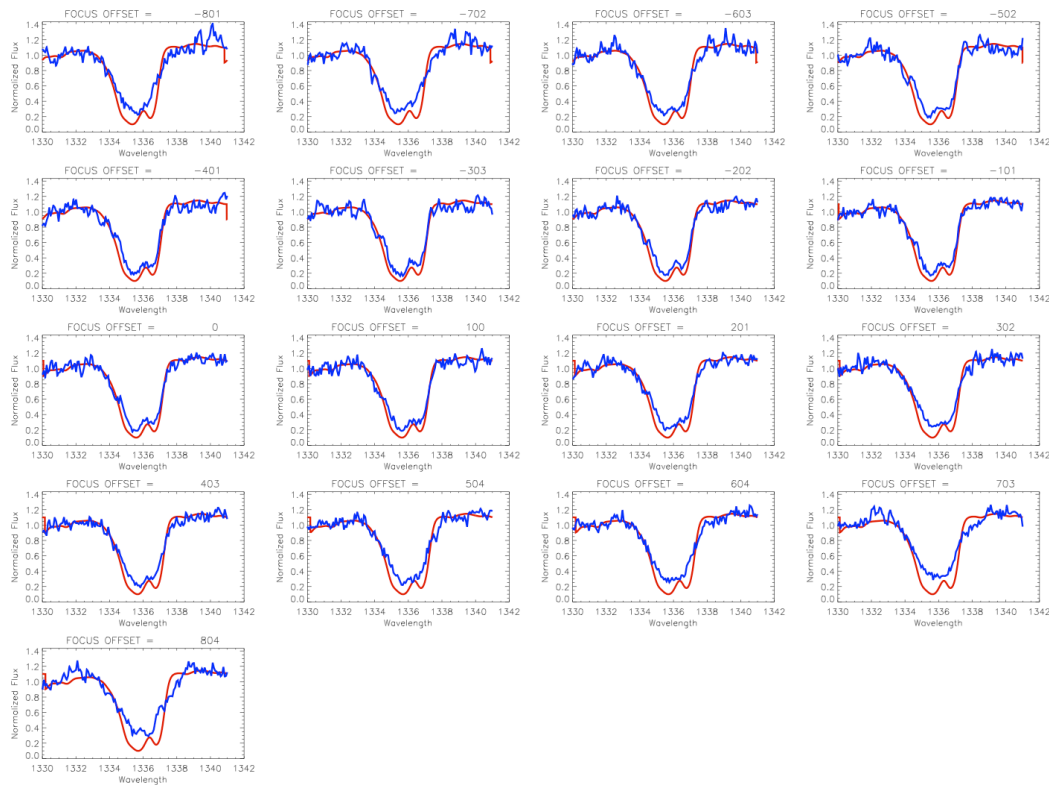


Figure 1. Closeup view of a pair of interstellar C II λ 1335 Å absorption lines in the COS G140L spectrum of AzV18 (shown in blue). The corresponding STIS E140M spectrum, convolved with the appropriate COS LSF model, is overlaid in red. The components are completely blended at the most extreme focus offsets.

The optimum focus setting is expected to vary with wavelength. Since the G140L spectra cover a significantly broader spectral range (\sim 1100 Å for Segment A at the 1105 Å central wavelength) than the G130M and G160M gratings (approximately

140 Å per segment), the optimal focus setting is expected to show a broader range across the G140L spectrum than for each of the medium resolution gratings. Prominent absorption lines across the AzV18 spectrum were fit with Gaussian profiles in CEDAR. Plots of the FWHM versus focus position were examined for each fitted prominent line. These produced considerably shallower focus curves than were obtained for G130M and G160M (Lennon et al. 2010), making identification of the minima in each curve difficult. In addition, it was found that the minimum of the focus curve occurred at large negative focus settings for some lines, and occurred at positive focus settings for others. No consistent trend with wavelength was found.

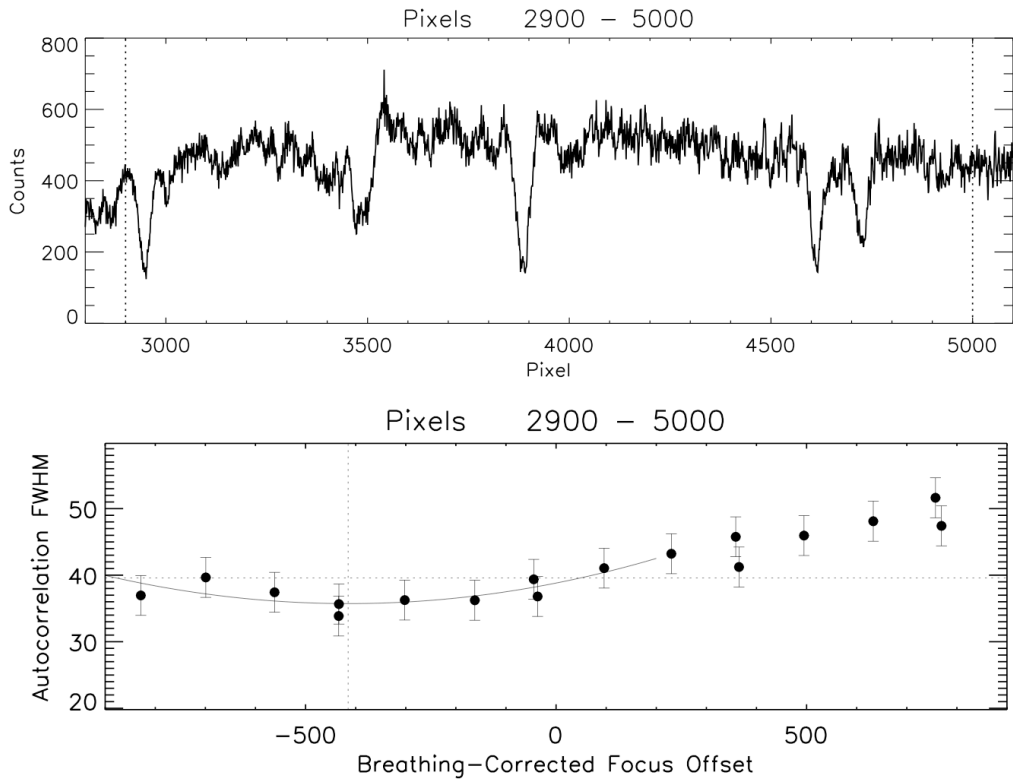


Figure 2. Top: G140L spectrum of Azv18, shown for the nominal focus offset. The dotted lines mark the spectral range used in the autocorrelation analysis. Bottom: The corresponding focus curve, shown with a quadratic fit to the data. The vertical dotted line marks the fitted optimum focus offset.

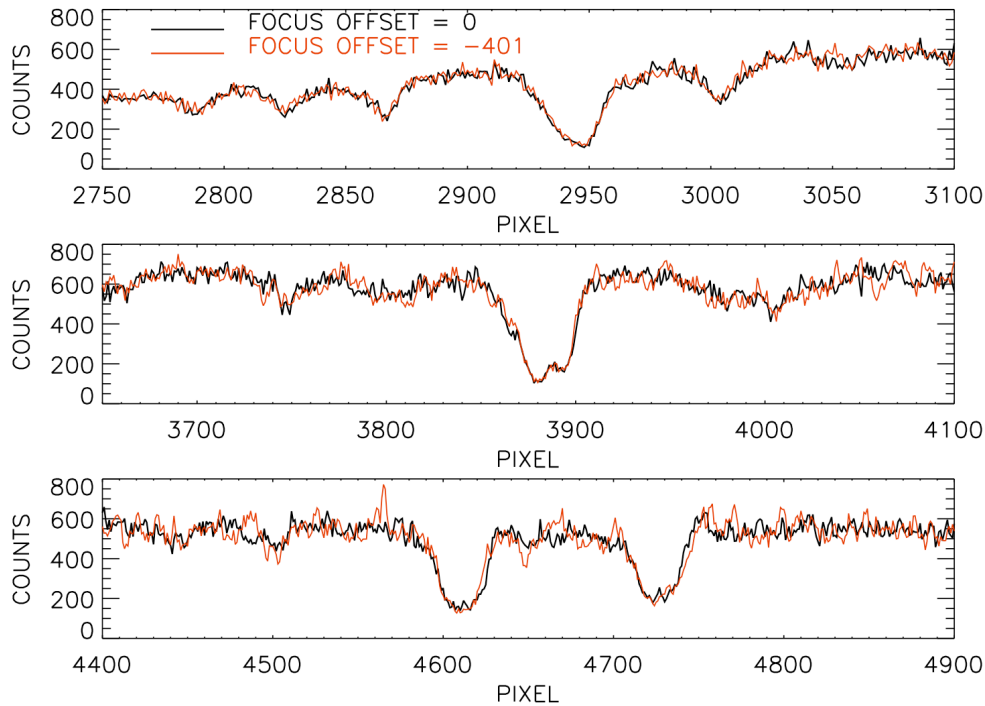


Figure 3. Closeup view of spectral lines in the G140L spectrum of Azv18, shown as a function of fully corrected pixel coordinates. Grid wires have been eliminated via flat fielding. Lines in the spectrum taken at a focus offset close to the optimum (l_{beg01edq}, at an offset of -401 steps) are not significantly narrower than lines taken at the nominal offset (l_{beg01elq}).

4.1 Autocorrelation Analysis

As an alternative method of finding the optimal focus position, an autocorrelation method was used similar to that described in Lennon et al. (2009). In this approach, the autocorrelation coefficient for an absorption feature is computed as a function of focus offset. The width of the resulting autocorrelation curve is determined by the widths of the lines in the spectrum. Broader lines yield broader auto-correlation function widths.

The autocorrelation was performed using a section of the spectrum between 1255 Å and 1430 Å (corresponding to pixels 2900 to 5000 in fully corrected detector coordinates). The resulting autocorrelation curve is shown in Figure 2, where the autocorrelation FWHM is plotted versus breathing-corrected focus offset. The error bars in autocorrelation FWHM were estimated for each point by assuming a 10% repeatability error, based on the scatter in autocorrelation widths obtained from the three exposures at nominal focus (l_{beg01e3q}, l_{beg01elq}, l_{beg01fdq}). The focus curve was fit with a quadratic function using data points within 500 steps of the nominal focus position. The minimum of the curve occurred at a focus offset of approximately -415 steps (or -785 in absolute focus). However, as seen in Figure 2,

this is not a strong result when the repeatability of the autocorrelation FWHM is taken into account. Due to the shallowness of the focus curve, the autocorrelation FWHM at zero offset is statistically indistinguishable from that at an offset of -415 steps. This result is confirmed in Figure 3, where little or no discernible difference can be seen between line profiles in the spectrum taken at nominal focus and that taken at an offset of -401 steps (the exposure closest to the derived optimal focus). This suggests that in contrast to the medium resolution gratings, determining an optimal focus setting for the G140L grating to within 50 focus steps is not feasible. For all practical purposes, then, the current focus position for the G140L grating at the 1105 Å central wavelength setting (and, by extension, the 1280 Å central wavelength setting) is already adequate.

5. Conclusions

An autocorrelation analysis of focus sweep data obtained for the COS G140L (1105 Å) grating during the Cycle 17 Supplemental Calibration Program shows a broad, shallow focus curve centered at approximately -785 steps in absolute focus, or -415 steps in focus offset from the nominal position. However, the focus curve for this grating is found to be broad and shallow, which combined with the uncertainty in repeatability make spectra taken at the nominal focus position indistinguishable from spectra taken close to the derived optimum offset. It is concluded that the current default focus position determined for the G140L grating during SMOV remains valid, and no further adjustment of the focus offset is recommended.

Acknowledgements

P.G. acknowledges helpful discussions with Daniel Lennon, Derck Massa and Cristina Oliveira. P. G. also wishes to thank Derck Massa for creating the one-dimensional G140L flat field template, and Stephane Béland for creating the two-dimensional G140L flat field from that template.

References

Lennon, D., et al. 2010, Instrument Science Report COS 2010-3, “COS FUV Focus Determination”